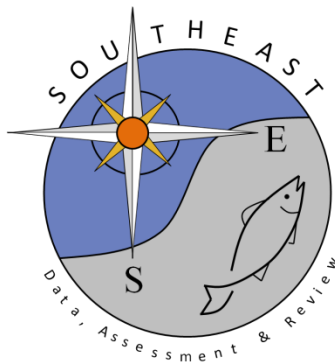Restricted connectivity for cobia Rachycentron canadum (Perciformes: Rachycentridae) in the Western Atlantic Ocean

Maria Raquel M. Coimbra, Emilly Benevides, Renata da Silva Farias, Bruno C. N. R. da Silva, Sara Cloux, Vicente Pérez-Muñuzuri, Manuel Vera, Rodrigo Torres

SEDAR95-RD-08

March 2024

ORIGINAL ARTICLE

FISHERIES OCEANOGRAPHY   WILEY

Restricted connectivity for cobia *Rachycentron canadum* (Perciformes: Rachycentridae) in the Western Atlantic Ocean

Maria Raquel M. Coimbra[1] 🔵 | Emilly Benevides[2] | Renata da Silva Farias[1] 🔵 | Bruno C. N. R. da Silva[1] | Sara Cloux[3] | Vicente Pérez-Muñuzuri[3] | Manuel Vera[4] 🔵 | Rodrigo Torres[2,5]

[1]Department of Fisheries and Aquaculture, Federal Rural University of Pernambuco, Recife, PE, Brazil

[2]Department of Zoology, Federal University of Pernambuco, Recife, PE, Brazil

[3]CRETUS Research Center, Nonlinear Physics Group, Faculty of Physics, University of Santiago de Compostela, Santiago de Compostela, Spain

[4]Department of Zoology, Genetics and Physical Anthropology, Faculty of Veterinary, University of Santiago de Compostela, Lugo, Spain

[5]Environmental Academic Department, Federal Technological University of Paraná, Paraná, Brazil

Correspondence
Maria Raquel M. Coimbra, Department of Fisheries and Aquaculture, Federal Rural University of Pernambuco, Recife, PE, Brazil.
Email: maria.rmcoimbra2@ufrpe.br

Abstract

Cobia (*Rachycentron canadum*) is a coastal pelagic migratory fish species of tropical and subtropical waters, where it is an important game fish and it has been commercially expanded in offshore aquaculture systems. Understanding population connectivity is of utmost importance to the sustainable use and conservation of aquatic resources, and information on genetic diversity and structure is key element in unraveling differentiation when no clear physical barriers exist. In the present study, cobia genetic diversity and structure were depicted using mitochondrial DNA cytochrome b sequencing and microsatellite genotyping in samples from the Southwestern Atlantic and showed that a major single population inhabits the southern hemisphere. Cytochrome b sequencing also suggested that the Indian Ocean is the center of origin for this species' diversification. A hierarchical analysis of AMOVA compared sampling locations from the Northwestern Atlantic (from a previous study) with the Southwestern ones using nine shared microsatellite markers. Differentiation among groups ($F_{CT} = 0.41$), Bayesian clustering analysis, and complementary ordination analyses (by discriminant analysis of principal components [DAPC] and factorial correspondence analysis [3D-FCA]) presented a clear separation between the two hemispheres, supported by a Lagrangian model that explained the ocean dynamics over larval retention on the Western Atlantic. Another genetic subgroup intermingled with the main Southwestern group may also exist further south, probably associated with the Vitória-Trindade Ridge and the local current systems. The distribution of this species in metapopulations is of extreme relevance for fisheries and fish hatcheries management in the Atlantic Ocean.

KEYWORDS
Atlantic Ocean, cobia, cytb, game fish, Lagrangian model, microsatellite, population structure, *R. canadum*, species diversification

1 | INTRODUCTION

Connectivity in marine populations is assumed as the geographic scale over which fish populations are connected or, at a more inclusive level, the flux of organisms, gametes, genes, disease vectors, and

Maria Raquel Moura Coimbra and Emilly Benevides should be considered joint first author.

nutrients between locations (Cowen & Sponaugle, 2009). The degree of connectivity depends on adult movements, larval dispersion, behavioral capabilities, climatic changes, geographic distances, and ocean currents dynamics, among others (Bashevkin et al., 2020; Gary et al., 2020; Leis et al., 2011). Nevertheless, higher homogeneity is expected in marine species, due to the large effective population size, high gene flow, and the absence of physical barriers to dispersal, especially during the larval planktonic stage (Palumbi, 1994; Sá-Pinto et al., 2012).

Information on marine connectivity is important to explore the genetic structure that arises in marine environments despite the larval dispersal potential of many species (Truelove et al., 2017). Therefore, seascape data associated with genomics can help to understand how population dispersion is affected (Bashevkin et al., 2020). In this sense, Lagrangian models have been used recurrently to explain larval dispersion and are useful to describe their trajectories (Sebille et al., 2018). These models are widely used in ocean dynamic transport studies, such as transport barriers (Huhn, Kameke, et al., 2012), eddy scales (Lumpkin et al., 2002), the influence of ocean dynamics on plankton blooms (Huhn, von Kameke, et al., 2012; Pérez-Muñuzuri & Huhn, 2010), or, more recently, for the dispersion of plastic debris in the ocean (Khoirunnisa et al., 2020; Sousa et al., 2021), among many other examples.

The cobia (*Rachycentron canadum*) is a migratory and coastal pelagic fish that occurs in the tropical and subtropical oceans of the globe, except in the eastern Pacific Ocean (Shaffer & Nakamura, 1989), and it is among the 100 world's top game fish species, according to Sport Fish Magazine (https://www.sportfishingmag.com/). The species is carnivorous, characterized as an opportunistic predator (Knapp, 1951; Meyer & Franks, 1996), with extremely high growth rates, reaching up to 2 m and weighing 60 kg in the natural environment (Chen et al., 2001; Franks et al., 1999). It is a usual solitary traveler, eventually forming small groups for spawning with a seasonal migratory behavior (Estrada et al., 2016). On the Western Atlantic Ocean, the species is distributed from Massachusetts, USA, to Argentina (Figueiredo & Menezes, 1980). In this region, spawning occurs throughout the year either inshore or offshore, with peaks between April and September for the Gulf of Mexico and South Carolina (Perkinson et al., 2019) and between February and April off Brazil (Hamilton et al., 2021).

Several genetic studies developed with *R. canadum* have demonstrated the efficiency of molecular markers in helping to understand population history, connectivity, diversity, and genetic structure (Divya et al., 2019; Gold et al., 2013; Perkinson et al., 2019). Gold et al. (2013) evaluated the genetic relationships of cobia from the North Atlantic (Gulf of Mexico and USA) based on nuclear and mitochondrial markers and suggested that in the Northwestern Atlantic, the species was organized as a homogenous population. Later, a refined study suggested that the Northwestern Atlantic is divided into two groups, one into the Gulf of Mexico and the second one above Florida (Perkinson et al., 2019).

Cobia is a species with an appeal for fishing exploitation, besides being widely cultivated in different parts of the world. Although it is distributed in tropical and subtropical waters, its genetic diversity and population structure have not been extensively investigated. In the Americas, cobia is a particularly important resource for sport fishing, and despite some previous studies on the Northwestern Atlantic, no attempts were made toward the Southwestern one. Therefore, testing the possible population structure for this species in the Western Atlantic is necessary for the elaboration of fisheries management plans, as well as for the logistics of breeding programs in aquaculture production, which is expanding into the Caribe and the Americas.

The present study aims to assess genetic diversity through a multilocus analysis and refine information on genetic structuring over ocean dynamics, using Lagrangian models in the Western Atlantic Ocean, and evaluate its implications for fishery management and aquaculture.

2 | MATERIAL AND METHODS

2.1 | Samples and genetic dataset

The sampling of fin clips and muscle tissues from 146 individuals of *R. canadum* was carried out at six landing locations in the Southwestern Atlantic Ocean of the Brazilian coast (Figure 1). Thirty of these were from Piauí (PI), 26 were from Ceará (CE), 25 were from the Rio Grande do the Norte (RN), 16 were from Paraíba (PB), 19 were from Bahia (BA), and 30 were from Espírito Santo (ES). The obtained tissues were stored in 96% ethanol and kept at −80°C.

To investigate the genetic structure along the Atlantic Ocean, a dataset from Gold et al. (2013), available at http://agrilife.org/gold/doc, containing 95 genotyped samples from the Northwestern Atlantic, 35 from Virginia (VA), 46 from Mississippi (MS), and 14 from Louisiana (LA), was used (Figure 1). From this same study, we also used four Northwestern Atlantic mitochondrial DNA haplotypes based on sequences of Cytochrome b (cytb) available in GenBank (accession numbers JX149559–JX149561, JX149563). For a transoceanic structure evaluation, we used 17 Indian Ocean cytb haplotype sequences from Divya et al. (2019) available in GenBank under the accession numbers KY712405–KY712421.

### 2.2 | Molecular procedures

2.2.1 | DNA extraction

DNA extraction was conducted using DNAEasy kit (QIAGEN) and integrity was evaluated using 1% agarose gel electrophoresis and quantified by NanoVue™ Plus Spectrophotometer (GE Healthcare).

2.2.2 | Microsatellite loci

Twelve microsatellite markers (Rca1D04, Rca1H04A, Rca1BA10, Rca1BH09, Rca1A11, Rca1B12, Rca1G05, Rca1BF06, Rca1BC06,
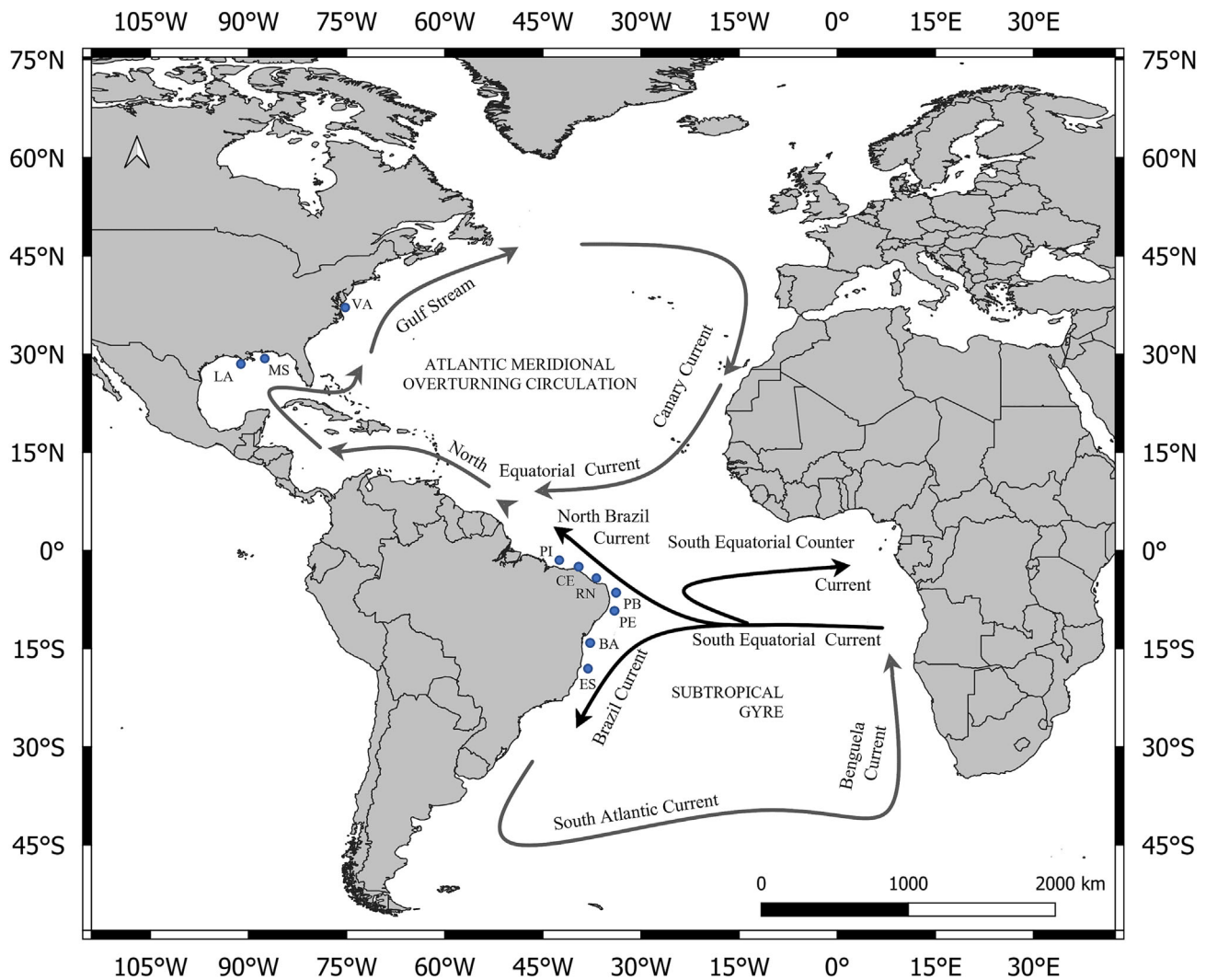
FIGURE 1 Map of approximate sampling locations (blue dots) for cobia *Rachycentron canadum* along the Western Atlantic Ocean (PI, Piauí; CE, Ceará; RN, Rio Grande do Norte; PB, Paraíba; and ES, Espírito Santo; and VI, Virginia; MS, Mississippi; and LA, Louisiana, extracted from Gold et al. (2013)). The main Atlantic Ocean currents are also shown with arrows.

Rca1C04, Rca1D11, and Rca1A04) previously described by Pruett et al. (2005) and Renshaw et al. (2005) were used to evaluate the genetic diversity of the samples from the Southwestern Atlantic Ocean (PI, CE, RN, PB, BA, and ES). The *forward primers* were *5′ end*-labeled with *fluorochromes*. Each PCR reaction with a final volume of 10 μL contained 20 ng DNA, 10 mM Tris–HCl pH 8.4, 50 mM KCl, 2.5 mM MgCl$_2$, 10 μM of each primer, 200 μM of each dNTP, and 1 U of *Taq* polymerase. The PCR amplification conditions were 94°C for 4 min, followed by 35 cycles of 94°C for 30 s, 45°C seconds at the appropriate annealing temperature (60–65°C), and 72°C for 1 min, plus final extension at 72°C for 40 min. Capillary electrophoresis separated PCR products on the ABI 3500 Genetic Analyzer (Applied Biosystems, USA) using GeneScan 600 LIZ v2.0 (Applied Biosystems, USA) as a molecular weight marker.

2.2.3 | mtDNA

The Cytochrome b (cytb) mitochondrial DNA (mtDNA) marker was amplified for all samples using the primers L14725 (Santos et al., 2003) and HMVZ16 (Smith & Patton, 1993). The PCR reaction for cytb included 10 pmol of each primer in 2X *Taq* Master Mix (Vivantis®, USA), 20 ng of DNA in a final volume of 20 μL. The PCR amplification consisted of an initial denaturation at 94°C for 3 min, followed by 30 cycles of denaturation at 94°C for 1 min, annealing at 45°C for cytb for 45 s, extension at 72°C for 90 s, followed by a final extension step at 72°C for 7 min. PCR products were purified with ExoSap-IT® and samples were sequenced on the ABI 3500 Genetic Analyzer automated sequencer (Applied Biosystems, USA), using the Big Dye® Terminator Cycle Sequencing Kit v3.1 (Applied Biosystems, USA) following the manufacturer's instructions.

2.3 | Genetic data analysis

2.3.1 | Microsatellite loci

To evaluate the genetic diversity for each of the six sampling locations at the Southwestern Atlantic Ocean, the genetic parameters such as number of alleles (N_a), expected (H_e) and observed (H_o) heterozygosities, inbreeding coefficient (F_{IS}), and the deviations of the Hardy–Weinberg Equilibrium (HWE) were obtained using the software GENEPOP 4.0 (Raymond & Rousset, 1995) for the 12 microsatellites. *P*-values of multiple tests were corrected by Bonferroni procedure (Rice, 1989).

The number of private alleles (N_p) was calculated using the GenAlEx 6.1 program (Peakall & Smouse, 2006), and to correct sample size, allelic richness (A_R) was estimated using FSTAT 2.9.4 (Goudet, 2003), by normalizing all locations to the smallest one. The Micro-Checker software (Oosterhout et al., 2006) was used to evaluate potential genotyping errors caused by stuttering, allelic dropouts, and the occurrence of null alleles (A_n).

To correct the biased comparison caused by differences in sample sizes, rarefaction curves of mean raw allelic diversity for the South Atlantic Ocean samples were estimated using the jackmsatpop function from the *PopGenKit* package (Paquette, 2012) in R v. 4.0.2 (R Core Team, 2020). For each population, 100 replicates were performed using a gradual increase of one individual until the true sample size of that location was reached. Although the curves do not provide statistical information, they are useful graphical tools to indicate whether sampling was sufficient to capture the allelic diversity of a location.

Global Wright's (F_{ST}) overall Southwestern sampling locations (Global F_{ST}) and pairwise population genetic differentiation values were calculated using Arlequin 3.5 (Excoffier & Lischer, 2010). Structure v. 2.3.4 (Pritchard et al., 2000) was used to identify the number and pattern of genetic clusters (K) among *R. canadum* Southwestern sampling locations. The Structure analysis was run under the admixture model, a burn-in period of 10,000 interactions, followed by Markov Chain Monte Carlo (MCMC) with 100,000 replicates, plus 10 replicates for each estimated K value (K = 1–10). The K value was obtained by the method proposed by Evanno et al. (2005) using Structure Harvester v. 0.6.7 software (Earl & vonHoldt, 2012). Second, the discriminant analysis of principal components (DAPC) (Jombart et al., 2010) was also used to investigate the population structure and was performed with the *Adegenet* package (Jombart, 2008) in R platform, v. 4.0.2 (R Core Team, 2020). This multivariate analysis is used to identify and describe genetic clusters while optimizing the variation among them. DAPC does not require populations to be in HWE or linkage disequilibrium loci (Jombart et al., 2010). Finally, a three-dimensional factorial correspondence analysis (3D-FCA) was carried out using GENETIX v. 4.05.2. (Belkhir et al., 2004). This analysis uses a minimal number of factors to explain the maximal amount of genetic variation.

Later, to evaluate the genetic structure of the *R. canadum* along the Western Atlantic Ocean, nine microsatellite markers (Rca1D04, Rca1H04A, Rca1BA10, Rca1BH09, Rca1B12, Rca1G05, Rca1BF06, Rca1C04, and Rca1D11) shared by the study of Gold et al. (2013) and the present one were used. Allele-size designations due to differences in laboratory routine and equipment used were adjusted using Gold et al.'s (2013) dataset as the baseline alleles for standardization. Under this hierarchical scenario and based on our results, as well as on Gold et al. (2013), two groups were considered: group 1 made by all the Southwestern sampling locations, and group 2, by the USA ones, Virginia, Mississippi, and Louisiana. Therefore, genetic differentiation associated with differences among sampling locations within groups (F_{SC}) and among groups (F_{CT}) was carried out by a hierarchical AMOVA, as well as the Bayesian analysis of structure (Structure), DAPC, and 3D-FCA.

Isolation by distance (IBD) was carried out using the Mantel test, performed with 10,000 permutations using the *ade4* package (Dray & Dufour, 2007) in the R platform, v. 4.0.2 (R Core Team, 2020). First, to evaluate the correlation between genetic and geographic distances, a standard Mantel test was conducted with sampling locations from the Northwestern and Southwestern Atlantic Oceans, and, later, a stratified Mantel test permuting locations within each group (Northwestern and Southwestern) was conducted.

Additionally, the population effective size number (N_e) was also calculated, under the hierarchical scenario of the Northwestern and Southwestern groups, for the nine common microsatellites, based on the linkage disequilibrium method using NeEstimator v1.3 (Do et al., 2014).

2.3.2 | mtDNA

The cytb sequences were edited in the CodonCode v.5.1.5 and aligned in MEGA v.5.2 (Tamura et al., 2011) using ClustalW (Thompson et al., 1994). To estimate the number and frequencies of haplotypes in the locations and the values of genetic diversity (haplotype and nucleotide), DNAsp v.5.10.00 (Librado & Rozas, 2009) was used. The haplotype network was built using the Network 4.5.6 program calculated by the median-joining algorithm (Bandelt et al., 1999). An additional haplotype network was built with cytb (712 bp) sequences including sequences from the Indian Ocean (980 bp), obtained by Divya et al. (2019) to investigate haplotype relationships at a transoceanic level. *Coryphaena hippurus* (GenBank accession number EF439196) was designated as the outgroup based on a phylogenetic study by Gray et al. (2009).

Global genetic differentiation (Φ_{ST}) between Southwestern sampling locations was estimated using Arlequin v.3.5 (Excoffier & Lischer, 2010). The demographic history was estimated using Tajima's D and Fu's Fs neutrality tests. Moreover, a third haplotype network was constructed with cytb, including sequences from the Northwestern Atlantic (352 bp) obtained from Gold et al. (2013), to evaluate the genetic structure between hemispheres.

2.4 | Lagrangian model

To study the connection between currents in the study area and larval dispersal, the MOHID-Lagrangian model (http://www.mohid.com) was used to simulate the trajectory of larvae in the Atlantic equatorial region and to estimate its accumulation along the coast. This model has been recently validated by Cloux et al. (2022) in a regional domain to simulate the dispersion of macroplastics from different sources. The model is forced with the currents obtained from Copernicus Marine Service (CMEMS) at https://marine.copernicus.eu/. This model used winds from European Centre for Medium-Range Weather Forecasts (ECMWF) and flow river discharges to obtain 3D currents. Only surface currents were used in this study. CMEMS model has a spatial horizontal resolution of 0.083°. Larvae, as considered Lagrangian points, are expected to follow the surface currents. The velocity field is interpolated from the hydrodynamic Eulerian velocity field to the tracer position to calculate the new position of the particle as

$$\frac{dx_i}{dt} = v_i(x_i, t) + D_i$$

where D_i is the subgrid-scale diffusion that accounts for unresolved physics such as mixed layer processes (Cloux et al., 2022). Three emission areas located along the Western Atlantic Ocean were used to simulate the dispersion at different latitudes. These emission areas were defined as polygons whose centroids are defined in Figure 4. In this type of emitter, the MOHID-Lagrangian assigns the emission points within the polygon at 9 km of spatial resolution. Therefore, the results are shown in relative terms of concentration, concerning the region of the ocean that registers a maximum accumulation.

Since the aim is to observe the potential dispersion of the different emission regions, and because the larval emission rate at the sampling points is unknown, a continuous emission was considered. Although the larval life is approximately 30 days (Salze et al., 2011), the 1.5-year (starting from January 2020) simulation period was considered to study the probability of dispersion after their life period and the season's effect.

3 | RESULTS

3.1 | Microsatellites

Initially, the sampling locations were treated as individual populations, and the genetic diversity was based on 12 microsatellite markers for each of the six locations in the Southwestern Atlantic Ocean (Table 1). Considering all six Southwestern locations, a total of 118 alleles were found within the 12 markers with an average number of alleles (N_a) per locus of 6.47, while the average allelic richness (A_R) per sampling site ranged from 5.72 to 5.98 (Table 1). Twenty-one private alleles were found: five in PI, five in CE, two in RN, one in PB, two in BA, and six in ES. Null alleles were found in the locus Rca1A11 for ES, but not systematically in all locations. No evidence was found of other

TABLE 1 Genetic diversity for wild cobia *Rachycentron canadum* from the Southwestern Atlantic Ocean (PI-Piauí, CE-Ceará, RN-Rio Grande do Norte, PB-Paraíba, BA-Bahia, and ES-Espírito Santo) based on 12 microsatellite loci and Northwestern and the Southwestern Atlantic oceans estimates based on nine microsatellites.

Samples	N	N_a	A_R	H_o	H_e	F_{IS}
12 microsatellites						
PI	30	6.92	5.98	0.642	0.646	0.001
CE	26	6.75	5.86	0.580	0.596	0.020
RN	25	6.42	5.72	0.620	0.624	−0.018
PB	16	5.75	5.75	0.609	0.596	−0.009
BA	19	6.00	5.72	0.680	0.633	−0.074
ES	30	7.00	5.89	0.614	0.599	−0.038
Nine microsatellites						
NW Atlantic	95	8.44	8.44	0.499	0.510	0.021
SW Atlantic	146	8.33	7.66	0.607	0.599	−0.019

Abbreviations: A_R, allelic richness; F_{IS}, inbreeding coefficient; He, expected heterozygosity; Ho, observed heterozygosity; N, number of individuals; Na, alleles number; NW, Northwestern; SW, Southwestern.

technical problems such as stuttering or allelic dropout. The rarefaction curves showed all locations following the same trajectory, indicating that similar allelic diversity was present among those samples (Figure S1) and that even though the sampling sizes were different among locations, they were sufficient to capture the allelic diversity of each location.

The average observed and expected heterozygosities (H_o and H_e), ranged from 0.580 in CE to 0.680 in BA and from 0.596 in CE to 0.646 in PI, respectively. Among the 72 of HWE tests (12 loci × 6 sampling locations), significant departures ($p < 0.05$) were observed for four loci, Rca1BA10 (for PB, $p = 0.0256$), Rca1A11 (for ES $p = 0.0069$), Rca1BC06 (for RN $p = 0.0257$), and Rca1C04 (for RN $p = 0.0428$); however, none of them remained significant after Bonferroni correction. Values of the inbreeding coefficient (F_{IS}) varied between −0.074 and 0.020.

A low level of global genetic differentiation among the six sampling locations was detected ($F_{ST} = 0.00947$, $p < 0.001$). The pairwise F_{ST} values for genetic differentiation of Southwestern sampling locations varied from 0 to 0.01455, being consistently significant ($p < 0.05$) between ES and all the other sampling locations (Table 2).

Among the K clusters tested (1–10) in the Bayesian clustering method (Structure), all Ks showed similar proportions of each cluster in each sampling location, with no genetic distinction between them (Figure S2). Although the ΔK method of Evanno indicated $K = 2$ (Figure S2) as the best K, due to caveats of this method concerning $K = 2$ (see Cullingham et al., 2020), and as the highest posterior probability ($P(K|X) = 0.9996$) was found in $K = 1$, this was adopted for simplicity (Figure 2a). The DAPC result indicated that most of the Southwestern sampling locations belong to a single population, with the sample of Bahia (BA) out of the range of the main distribution (Figure 2b). Likewise, the 3D-FCA result showed a centered

	PI	CE	RN	PB	BA	ES
PI	-					
CE	0.00671	-				
RN	0.00298	0.00494	-			
PB	0.00896	0.01170*	0.00656	-		
BA	0.00743*	0.00646	0.00455	0.00769	-	
ES	0.01383*	0.01455*	0.01403*	0.01384*	0.01438*	-

TABLE 2 Estimated pairwise F_{ST} (below diagonal) for samples of cobia *Rachycentron canadum* from the Southwestern Atlantic (Piauí, Ceará, Rio Grande do Norte, Paraíba, and Espírito Santo) based on 12 microsatellites.

Abbreviations: CE, Ceará; ES, Espírito Santo; PB, Paraíba; PI, Piauí; RN, Rio Grande do Norte.

*Significant values ($p < 0.05$).
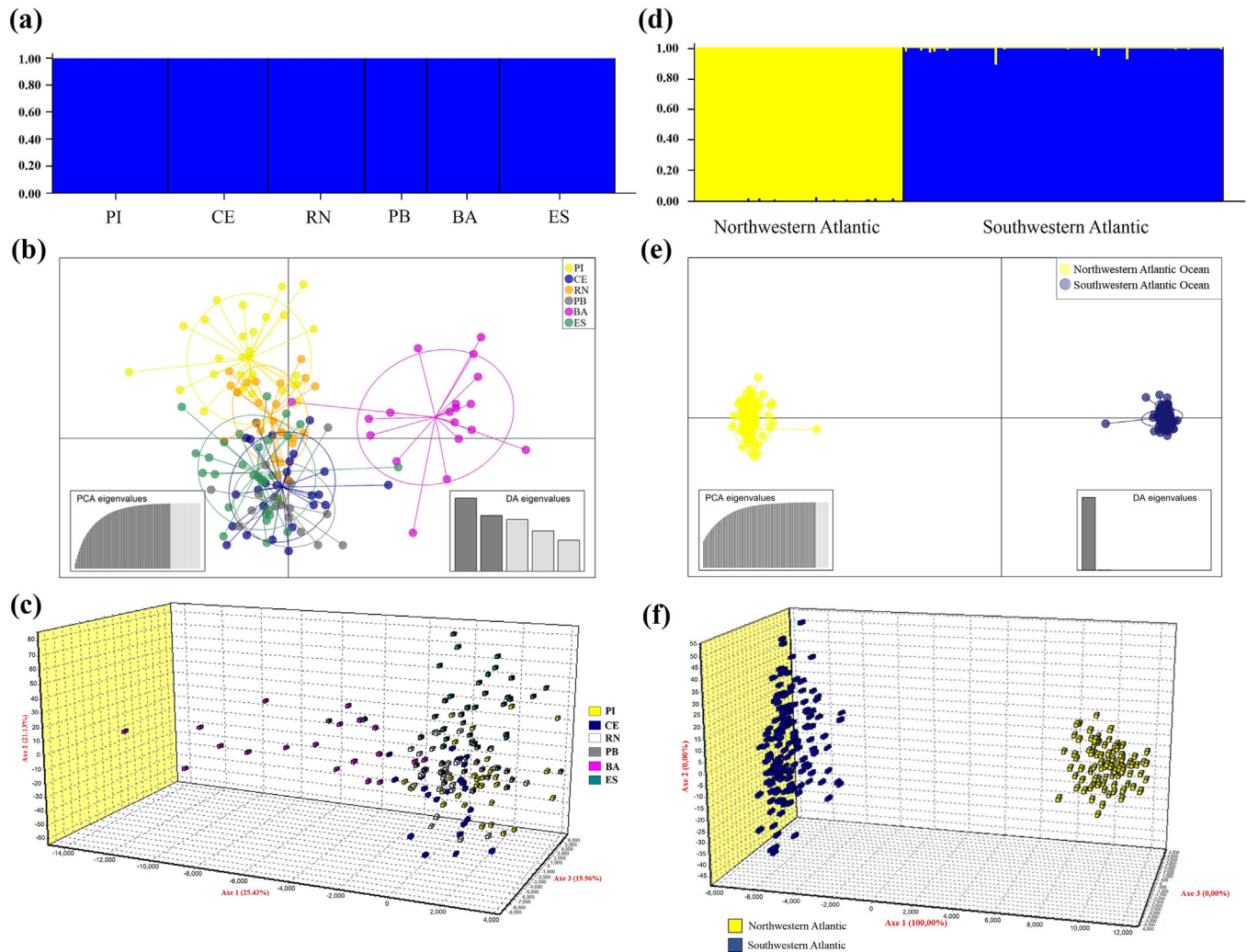
FIGURE 2 Genetic structure of cobia *Rachycentron canadum* wild samples from Southwestern Atlantic (PI, Piauí; CE, Ceará; RN, Rio Grande do Norte; PB, Paraíba; and ES, Espírito Santo), evaluated based on allele frequencies of 12 microsatellite loci on the left by three approaches: (a) attributions of genotypes by structure, where each vertical bar represents a different individual and the length is proportional to the inferred group, cluster 1 (blue); (b) scatterplot of the discriminant analysis of principal components (DAPC); and (c) three-dimensional factorial correspondence analysis (3D-FCA). On the right, the genetic structure of cobia wild samples from Northwestern and Southwestern Atlantic groups based on nine microsatellites, where each vertical bar represents a different individual and the length is proportional to the inferred group (d), cluster 1 (blue) and cluster 2 (yellow). Scatterplot of DAPC for Northwestern and Southwestern sampling locations (e); and (f) 3D-FCA for Northwestern and Southwestern sampling locations.

concentration of samples, except for the sampling location of Bahia (BA). The 3D-FCA showed that a total of 66.52% of variance accounted for the first three factors (Figure 2c).

Taking these results into account, a hierarchical scenario was created using the two groups, the Northwestern and Southwestern, carried out with nine common microsatellite loci genotyped by Gold

et al. (2013) and by the present study (Table 3). The hierarchical AMOVA showed an F_{CT} value of 0.4061 and 40.61% of the variance could be explained by differences among the two groups, while 58.86% by differences within sampling sites (F_{ST}).

Under this hierarchical scenario, the ΔK method of Evanno indicated $K = 2$ as the best$K$ (Figure S3) and the highest posterior probability $P(K|X) = 0.5$ was found for $K = 2$ and $K = 3$. Because both Ks showed the same result, a clear distinction between the two hemispheres with equal proportions for each cluster, we have adopted $K = 2$ for simplicity (Figure 2d). DAPC and 3D-FCA resulted in the same clustering pattern showing a clear separation between Northwestern and Southwestern Atlantic groups (Figure 2e,f). The 3D-FCA showed that a total of 88.3% of variance accounted for the first three factors (Figure 2f).

Although the IBD standard analysis indicated a strong positive correlation (0.974, $p = 0.008$) between genetic and geographic distances, the stratified Mantel tests permuting locations within Northwestern ($r = -0.378$, $p = 0.495$) and Southwestern ($r = -0.423$, $p = 0.947$) groups did not support IBD for associations of locations between the two groups.

The effective population size for the samples grouped as Northwestern and Southwestern Atlantic was $Ne = \infty$ (95% $CI = 244.4 - \infty$) and 15,328.3 (95% $CI = 355.8 - \infty$), respectively (Table 4).

3.2 | mtDNA

A total of 143 sequences for the South Atlantic samples were obtained for the cytb marker. After trimming ambiguous ends, the final length of the aligned sequences was 712 bp (Table 5). Among these sequences, a total of eight different haplotypes (h) were found. The total haplotype diversity (hd) was 0.4, and the nucleotide diversity (π) was 0.00075. The greatest haplotype diversity was found in PI (hd = 0.513; h = 7), while the lowest value was found in PB (hd = 0.125; h = 2).

Tajima's D and Fu's Fs neutrality tests were negative for the cytb. However, some of them were significant. The values for the neutrality tests within each sampling location can be seen in Table 5. A low global $\Phi_{ST} = 0.02467$ was detected, although significant ($p < 0.05$).

The haplotype network (Figure 3a) with the Southwestern sampling locations showed a high frequency (76.7%, 112/146) of a central haplotype (H1), with two exclusive haplotypes observed in PI, the northernmost location.

TABLE 5 Summary of diversity and neutrality tests for a fragment of 712 bp of the cytochrome b in cobia (*Rachycentron canadum*) from the Southwestern Atlantic (PI- Pìauí, CE- Ceará, RN- Rio Grande do Norte, PB- Paraíba, BA- Bahia, and ES-E Espírito Santo).

Samples	n	h	hd	π	D	Fs
PI	30	7	0.513	0.0012	−1.8264*	−3.0257*
CE	26	3	0.280	0.0004	−0.9598	−1.0465
RN	24	4	0.431	0.0009	−1.5177*	−0.8528
PB	16	2	0.125	0.0002	−1.1622	−0.7001*
BA	18	4	0.471	0.0007	−1.1313	−1.5963*
ES	29	3	0.431	0.0006	−0.2478	−0.1712

Abbreviations: D, Tajima's test; Fs, Fu's Fs test; h, number of haplotypes; hd, haplotype diversity; n, sample size; Π, nucleotide diversity.
*$p < 0.05$.

TABLE 3 AMOVA of microsatellite markers of *Rachycentron canadum* in the Western Atlantic Ocean based on nine microsatellites.

Hierarchical AMOVA	d.f.	Variance components	% variation	F-statistics
Among NW and SW Atlantic Ocean	1	1.74552 V_a	40.61	$F_{CT} = 0.4061$*
Among sampling locations within NW and SW Atlantic Ocean	7	0.02296 V_b	0.53	$F_{SC} = 0.0089$**
Within sampling locations	471	2.53071 V_c	58.86	$F_{ST} = 0.4114$**
Total	479	4.29865	100	

Abbreviations: d.f., degree of freedom; F_{CT}, variation among Northwestern and Southwestern groups; F_{SC}, variation among sampling locations within groups; F_{ST}, variation within sampling locations; Va, Vb, Vc: Number of variance components.
*$p < 0.05$.**$p < .001$.

TABLE 4 Effective population sizes (Ne) of *Rachycentron canadum* locations from the Northwestern Atlantic and the Southwestern Atlantic oceans estimates based on the linkage disequilibrium method and using nine microsatellites.

Population	N_e−linkage disequilibrium			
	The lowest allele freq used	N_e	95% CI lower	95% CI upper
NW Atlantic	0.05	∞	244.4	∞
	0.02	1306.1	219.2	∞
	0.01	∞	740.8	∞
SW Atlantic	0.05	15,328.3	355.8	∞
	0.02	2002	391.7	∞
	0.01	1599.9	407.2	∞

Abbreviations: NW, Northwestern; SW, Southwestern.
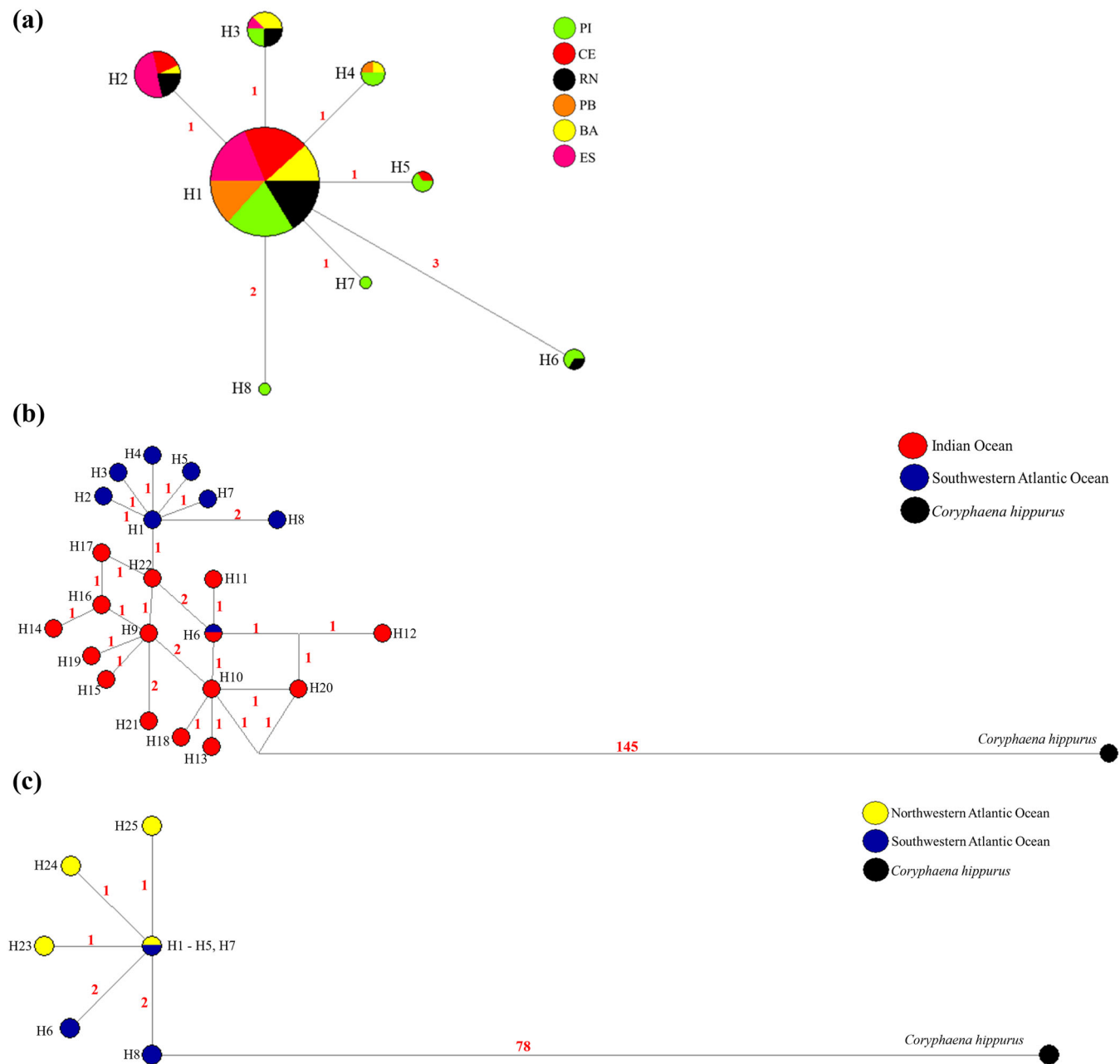
FIGURE 3 *Rachycentron canadum* haplotype network of cytb using the median-joining method. (a) A 712-bp fragment sequenced in six sampling sites in the Southwestern Atlantic Ocean. The numbered circles represent the haplotypes (H)and the sizes of the circles correspond to the frequencies of haplotypes; (b) a 712-bp fragment sequenced in six sampling sites in the Southwestern AtlanticOcean (blue)and four sampling sites (red) in the Indian Ocean (Divya et al., 2019), where the frequency of haplotypes is not represented; and (c) a 352-bp fragment sequenced in six sampling sites in the Southwestern Atlantic Ocean (blue) and three sampling sites (yellow) in the Northwestern Atlantic Ocean (Gold et al., 2013), where the frequency of haplotypes is not represented. Previous haplotypes from "a" network have collapsed as H1, which is the most frequent haplotype in the Southwestern, while H23 is the most frequent in the Northwestern.

When our cyt-b sequences were aligned with those from the Indian Ocean with 712 bp length (Divya et al., 2019), the network haplotype (Figure 3b) also presented a star-like shape with 22 haplotypes, being seven exclusives from the Southwestern Atlantic Ocean, 14 privates to the Indian Ocean, and one (H6) shared by both regions. The haplotype H10, from the Indian Ocean, was the closest one to the outgroup.

For investigating genetic structure using mtDNA, a haplotype network constructed with 352 bp sequences from the Southwestern and Northwestern Atlantic Oceans by Gold et al. (2013) showed a star-like shape with seven haplotypes (Figure 3c). Out of these, two were exclusive to the Southwestern, four to the Northwestern, and one shared by both hemispheres. It is of note that this 352 bp cytb sequence could not be used for comparing the three sets of data

—WILEY

(Southwestern Atlantic, Northwestern Atlantic, and Indian Oceans) in a single haplotype network, as too much information would have been lost. Because of that, previous haplotypes (H2, H3, H4, H5, and H7) from Figure 3a, collapsed as H1 (Figure 3c).

3.3 | Larvae dispersion

Larvae Lagrangian dispersion is shown in Figure 4 after a 1.5-year simulation for three different emission areas on the eastern American coast. The first emission area, located in the northern Gulf of Mexico (Figure 4a), covering New Orleans's south coast (from 91.37°W, 28.05°N to 87.7°W, 28.05°N), shows that the Lagrangian particles emitted here flow through the Florida Strait to join the Gulf Stream, giving rise to the Atlantic Meridional Overturning Circulation (AMOC) flow.

Results are also shown for the northwestern coast of Brazil. Here two strategic points were selected to analyze the influence of the Amazon River and the distance to the Equator in the larvae transport. The first emission area extends from Turiaçu Bay (45.19°W, 1.29°S) to approximately Fortaleza (38.42°W, 3.58°S), covering the São Marcos Bay (39.22°W, 2.89°S). With this emitter, south of the mouth of the Amazon, we intended to test whether this river could function as a transport barrier (Huhn, Kameke, et al., 2012). As shown in Figure 4b, particles emitted from this source move in a northwesterly

direction along the coast to equatorial latitudes where they begin to disperse eastward following the south equatorial countercurrent. However, a small percentage of particles can cross the Equator toward the northern hemisphere, reaching the Caribbean Sea and the Gulf of Mexico and rejoining the AMOC. During the 18-month simulation, seasonal fluctuations of the Amazon River flow discharges were considered by the CMEMS model, which may explain the large larvae dispersion observed in the South Atlantic region.

Finally, an emission point was located below Cape São Roque (35.25°W, 5.48°S) to observe larval behavior at latitudes below the equator. Specifically, this last emitter extends from the Maceió coast (35.67°W, 9.69°S) to the Orojo River mouth (38.94°W, 13.84°S), covering the mouth of the San Francisco River (36.39°W, 10.52°S). Figure 4c demonstrated that the particles can follow two paths: either a northern circulation near the coastline that, once reaching Cape San Roque, will follow a dynamic identical to that described in Figure 4b, or the particles emitted in this region may also couple to the Brazil Current (BC) initiating a southward transport.

4 | DISCUSSION

The present results showed two genetic groups in *R. canadum* for the Western Atlantic Ocean: one in the Northwestern (Northern Gulf of
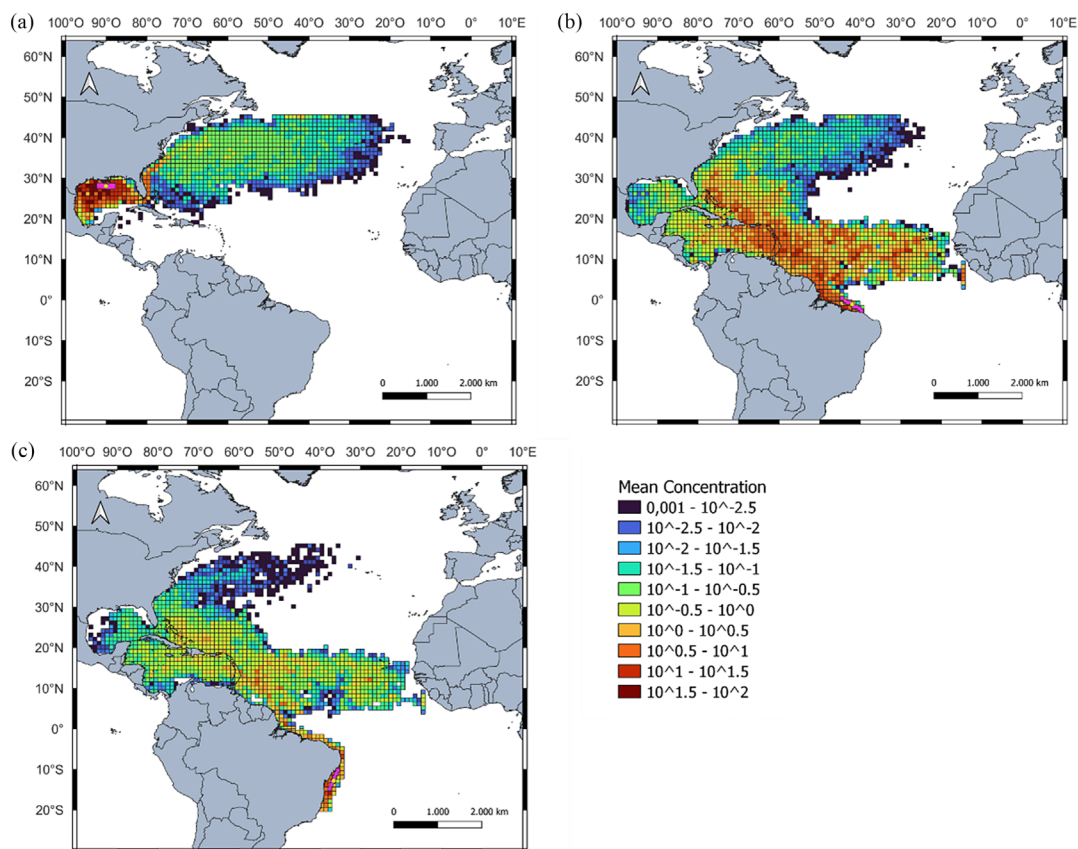
FIGURE 4 Larvae concentrations after a 1.5-year Lagrangian simulation for three different emission areas at the eastern American coastline. Centroids (yellow dots) of the initial emission coordinates are: 90.08°W to 28.04°N (a), 41.99°W to 1.12°N (b), and 36.62°W to 12.81°S (c).

Mexico and US Northwestern) and the other in the Southwestern, extending throughout the coast of Brazil. We propose that this difference might be, at some level, influenced by the oceanographic current system over larval retention.

4.1 | Genetic diversity along the Southwestern Atlantic Ocean

This is the first study to depict the genetic diversity of *R. canadum* in the Southwestern Atlantic. Microsatellite markers revealed an average genetic diversity in terms of H_o (0.62), H_e (0.62), and N_a (6.47) that were far below those values described for marine species (heterozygosity = 0.79, mean alleles per locus = 20.6) by DeWoody and Avise ([2000](#)). However, our values for H_o, H_e, N_a, and A_R (5.82) were higher than those described by Gold et al. ([2013](#)), for samples taken from the Northwestern Atlantic (two locations in the Gulf of Mexico and another farther up, off Virginia) and genotyped for 28 microsatellites, H_o (0.44), H_e (0.45), N_a (8.4), and A_R (4.58), but lower than those described in another study of cobia, with samples taken only off Virginia and off North and South Carolina states, H_o (0.747), H_e (0.749), and N_a (15.4). Nevertheless, when the Southwestern and Northwestern Atlantic samples were analyzed using only the nine common microsatellite markers (Table [1](#)), this genetic diversity difference decreased. Our results were also lower than those from the Indian Ocean, H_o (0.76), H_e (0.73), and N_a (11.3), as described by Divya et al. ([2019](#)), and far below those reported for the Indo-Pacific region (the Gulf of Thailand and the Andaman Sea), where N_a was 17.7 and H_e varied between 0.829 and 0.854, while A_R ranged between 11.9 and 13.1 (Phinchongsakuldit et al., [2013](#)).

This low genetic variability was also evidenced by mitochondrial data (cytb, 712 bp), as out of eight haplotypes detected in the Southwestern Atlantic, one (H1) was present in 76.71% (112/146) of the individuals, supporting a founder effect hypothesis derived from a main maternal lineage. This hypothesis is supported by the fact that, in the Indian Ocean, the number of haplotypes was almost double (14 haplotypes) that of the Southwestern Atlantic, and the Indian haplotype (H10) was the closest one to the outgroup species (*C. hippurus*), suggesting this is likely to be the region for the initial diversification of this group.

Despite of the low genetic diversity compared to other regions, the Southwestern Atlantic group rendered point estimates values of *Ne* away above 500, while infinite estimates were found in the Northwestern group. According to Waples and Do ([2010](#)), these infinite values may represent sampling errors. However, in both groups, the lower bound of the confidence interval (CI) values were finite, which, based on these authors, could provide useful information on the reasonable limits of *Ne* that were very close or higher than 250, considered as a minimum number to avoid inbreeding from a conservation perspective (Frankham et al., [2014](#)).

4.2 | The genetic structure along the Western Atlantic Ocean

Considering the results on microsatellite and mtDNA data that indicated a single population in the Southwestern Atlantic Ocean, a hierarchical scenario was carried out by comparing two groups of sampling locations (Northwestern and Southwestern Atlantic) genotyped for nine common microsatellites: three sampling locations available from Gold et al. ([2013](#)) and the six locations from the present study. Two well-structured groups were found by different approaches: through F_{CT}, Bayesian analysis, DAPC, and 3D-FCA (Figure [2](#)). As no standard sample set for a precise allele size standardization was available between the two laboratories (Gold et al., [2013](#) and ours), these results should be taken with caution. Nevertheless, mtDNA results confirmed the microsatellite findings as the haplotype network of cytb (Figure [3c](#)) showed only one common haplotype between the North and Southwestern Atlantic Oceans. According to Gold et al. ([2013](#)), the most common haplotype (80%, 12/15) in the Northwestern Atlantic (JX149559), which corresponds to H23 (Figure [3c](#)), is not present in the southern hemisphere. Yet the most common haplotype in the Southwestern Atlantic was H1, which was present at a very low frequency (1/15) in the Northwestern, suggesting limited gene flow between these groups. These results suggested that at least two genetic populations of *R. canadum* exist along the Western Atlantic, one in the northern hemisphere and another in the southern one.

Most pelagic fish reproduces via the larval phase, and in many cases, these larvae are carried out by ocean currents. However, the scale of this transportation is probably much smaller than accepted. Likewise, self-recruitment is limited to small areas where local-scale physical processes might play an important role in larval transport (Pineda et al., [2007](#)).

The South Equatorial Current (SEC) is an east–westward current that when it reaches the Brazilian shelf region divides into the North Brazil Current (NBC), an equatorward current that continues to the upper ocean and returns to the AMOC, and into the BC, a poleward current (Marcello et al., [2018](#)). The NBC separates from the Brazil coastline and retroflects to join the North Equatorial Countercurrent; however, this retroflection seasonally weakens and allows the nutrient-rich outflow from the Amazon River to be transported toward the Caribbean Sea by NBC (Fratantoni & Richardson, [2006](#); Muller-Karger et al., [1988](#)). A loop current system around the Gulf brings warm waters from Caribe through the Yucatan Channel and northward to the Atlantic Ocean, joining the Gulf Stream (Gopalakrishnan et al., [2013](#); Gordon, [1967](#); Welsh & Masamichi, [2000](#)), which is an integral part of the North Atlantic subtropical gyre circulation (Candela et al., [2019](#)).

According to these predominant current systems, larvae originated from inshore or from the continental Brazilian shelf can be driven to either the north or the south, depending on the location. On the other hand, larvae from the Gulf of Mexico apparently could only be driven to the north.

The Lagrangian results showed that particles released in southern latitudes can flow northward, southward, and eastward as shown in Figure 4, consistent with the upper-level circulation in this area, as the SEC splits into two branches upon reaching the Brazilian coast. Therefore, larvae emitted at equatorial latitudes may be carried northward along the NBC or be transported southward along the BC, with no obstacles. There may also be a longitudinal shift eastward along the South Equatorial Counter Current. Nevertheless, the opposite movement, that is, of larvae from the Gulf of Mexico, toward Central America and Brazil is not likely to happen. Particles released in more northern latitudes are not able to cross the equator (Figure 4c). It remains to be investigated if the Caribbean Sea is a transition zone, either gradual or sharp, which requires additional sampling, or if it belongs to the Southwestern group since the NBC could drive larvae up to this area.

Apart from that, two groups may exist in the Northwestern Atlantic Ocean, according to Perkinson et al. (2019). Using tagging and genetic data, they suggested that one group is found in the Gulf of Mexico up to Florida and a second one from Georgia farther up to Virginia. They also suggested that the distribution of eggs and larvae would be impacted by a temperature transition zone from a temperate to a subtropical climate. Interestingly, among the Brazilian sampling locations, the two southernmost ones (BA and ES) seemed to be separating from the remaining locations. Samples taken off Espirito Santo showed consistent significant pairwise FST values among all locations. Yet samples taken off BA presented a dispersion about the central tendency in the 3D-FCA geometrical association, as also belonged to a separate group in the DAPC method. Vessels from these two southernmost locations (BA and ES) may share the same fishing grounds but land in different seafood markets, which would explain the similar tendency. In this case, unlikely proposed by Perkinson et al. (2019) for the North American second group, the suggested divergence would be a result not of a transition into a subtropical zone but of the current system itself. The abovementioned bifurcation of the SEC seasonally shifts between 13°S, in summer, and 17°S, in winter. When the bifurcation latitude moves to the north, the NBC transport decreases, while the BC increases (Rodrigues et al., 2007). Cobia larvae from that region might be carried predominantly southward. Moreover, at 20.5°S, the BC interacts with an obstacle, a submarine chain reaching up to 30 m below the surface, the Vitória-Trinidad Ridge. This encounter along with opposite southern cold currents forms mesoscale eddies up and downstream the ridge that exposes nutrient-rich waters and enhances primary productivity below the mixed layer (Napolitano et al., 2021). This region represents a barrier to gene flow to many species that either resume their southern limit or show divergence in genetics in this area, including oysters, crustaceans, polychaetes, and red macroalgae (Martins et al., 2021). It is feasible that being close to this ridge, the south of Bahia coast (BA) and Espírito Santo (ES) might belong to a southern emerging subgroup.

These findings on the structure of cobia populations under the influence of surface current system on larval retention in the Western Atlantic Ocean bring important information not only to fishery management of this important game fish species but also to fish hatchery management. The future of commercial production of cobia relies on offshore aquaculture, which provides adequate environmental conditions for this species with large operating systems in the Americas (Benetti et al., 2021), from Mexico to Brazil, including Caribe. Growout offshore aquaculture needs to be concerned about fish escapees as those could threaten the survival of the indigenous conspecifics and promote introgression from fish from distinct genetic origins. Moreover, as fingerling production for this species can be challenging (Benetti et al., 2008), hatcheries should ensure the genetic origin of the fingerlings to grow out farmers, since this species is distributed as metapopulations in the Western Atlantic Ocean.

5 | CONCLUSION

We concluded that cobia from the Western Atlantic Ocean is less genetically diverse than that from the Indo-Pacific Ocean, suggesting that this region must be the center of this species' diversification. Both types of markers (mtDNA sequencing and microsatellite genotyping) used indicated the existence of two genetic groups of cobias in the Western Atlantic Ocean, one in the northern and another in the southern hemisphere. This genetic divergence seems to rely on the current system of the Gulf of Mexico, which is likely to limit larval dispersal toward the Southwestern. Additionally, in the southwestern group, a subgroup is perhaps emerging under the poleward BC prevalence and gene flow barrier caused by the Vitória-Trinidad Ridge.

CONFLICT OF INTEREST STATEMENT

The authors declare that they have no known competing financial interests or personal relationships that could have appeared to influence the work reported in this paper.

DATA AVAILABILITY STATEMENT

The data that support the findings of this study are available from the corresponding author upon reasonable request.

ORCID

Maria Raquel M. Coimbra https://orcid.org/0000-0002-2680-8783
Renata da Silva Farias https://orcid.org/0000-0003-4082-3186
Manuel Vera https://orcid.org/0000-0003-1584-6140

REFERENCES

Bandelt, H. J., Forster, P., & Röhl, A. (1999). Median-joining networks for inferring intraspecific phylogenies. *Molecular Biology and Evolution*,

16(1), 37–48. https://doi.org/10.1093/oxfordjournals.molbev.a026036

Bashevkin, S. M., Dibble, C. D., Dunn, R. P., Hollarsmith, J. A., Ng, G., Satterthwaite, E. V., & Morgan, S. G. (2020). Larval dispersal in a changing ocean with an emphasis on upwelling regions. *Ecosphere*, 11(1), e03015. https://doi.org/10.1002/ecs2.3015

Belkhir, K., Goudet, J., Chikhi, L., & Bonhomme, F. (2004). Genetix 4.05, logiciel sous Windows™ pour la génétique des populations. In *Laboratoire Génome, Populations, Interactions*. Université de Montpellier II.

Benetti, D. D., Sardenberg, B., Welch, A., Hoenig, R., Orhun, M. R., & Zink, I. (2008). Intensive larval husbandry and fingerling production of cobia *Rachycentron canadum*. *Aquaculture*, 281(1–4), 22–27. https://doi.org/10.1016/j.aquaculture.2008.03.030

Benetti, D. D., Suarez, J., Camperio, J., Hoenig, R. H., Tudela, C. E., Daugherty, Z., McGuigan, J. C., Mathur, S., Anchieta, L., Buchalla, J. A., Marchetti, D., Fiorentino, J., Buchanan, J., Artiles, A., & Stieglitz, J. D. (2021). A review on cobia, *Rachycentron canadum*, and aquaculture. *Journal of the World Aquaculture Society*, 52(3), 691–709. https://doi.org/10.1111/jwas.12810

Candela, J., Ochoa, J., Sheinbaum, J., Lopez, M., Perez-Brunius, P., Tenreiro, M., Pallaàs-Sanz, E., Athié, G., & Arriaza-Oliveros, L. (2019). The flow through the Gulf of Mexico. *Journal of Physical Oceanography*, 49(6), 1381–1401. https://doi.org/10.1175/JPO-D-18-0189.1

Chen, Y. H., Su, M. S., & Liao, I. C. (2001). Challenges and strategies of cage aquaculture development in Taiwan. In *Book of abstracts, aquaculture 2001*. World Aquaculture Society.

Cloux, S., Allen-Perkins, S., de Pablo, H., Garaboa Paz, D., Montero, P., & Pérez-Muñuzuri, V. (2022). Validation of a Lagrangian model for large-scale macroplastic tracer transport using mussel-peg in NW Spain (Ría de Arousa). *Science of the Total Environment*, 822, 153338. https://doi.org/10.1016/j.scitotenv.2022.153338

Cowen, R. K., & Sponaugle, S. (2009). Larval dispersal and marine population connectivity. *Annual Review of Marine Science*, 1, 443–466. https://doi.org/10.1146/annurev.marine.010908.163757

Cullingham, C. I., Miller, J. M., Peery, R. M., Dupuis, J. R., Malenfant, R. M., Gorrell, J. C., & Janes, J. K. (2020). Confidently identifying the correct K value using the ΔK method: When does K= 2? *Molecular Ecology*, 29(5), 862–869. https://doi.org/10.1111/mec.15374

DeWoody, J. A., & Avise, J. C. (2000). Microsatellite variation in marine, freshwater and anadromous fishes compared with other animals. *Journal of Fish Biology*, 56, 461–473. https://doi.org/10.1111/j.1095-8649.2000.tb00748.x

Divya, P. R., Linu, J., Mohitha, C., Kathirvelpandian, A., Manoj, P., Basheer, V. S., & Gopalakrishnan, A. (2019). Deciphering demographic history and fine-scale population structure of cobia, *Rachycentron canadum* (Pisces: Rachycentridae) using microsatellite and mitochondrial markers. *Marine Biodiversity*, 49(1), 381–393. https://doi.org/10.1007/s12526-017-0817-x

Do, C., Waples, R. S., Peel, D., Macbeth, G. M., Tillett, B. J., & Ovenden, J. R. (2014). NeEstimator v2: Re-implementation of software for the estimation of contemporary effective population size (Ne) from genetic data. *Molecular Ecology Resources*, 14(1), 209–214. https://doi.org/10.1111/1755-0998.12157

Dray, S., & Dufour, A. B. (2007). The ade4 package: Implementing the duality diagram for ecologists. *Journal of Statistical Software*, 22(4), 1–20. https://doi.org/10.18637/jss.v022.i04

Earl, D. A., & vonHoldt, B. M. (2012). STRUCTURE HARVESTER: A website and program for visualizing STRUCTURE output and implementing the Evanno method. *Conservation Genetics Resources*, 4(2), 359–361. https://doi.org/10.1007/s12686-011-9548-7

Estrada, U. R., Yasumaru, F. A., Tacon, A. G., & Lemos, D. (2016). Cobia (*Rachycentron canadum*): A selected annotated bibliography on aquaculture, general biology and fisheries 1967–2015. *Reviews in Fisheries Science & Aquaculture*, 24(1), 1–97. https://doi.org/10.1080/23308249.2015.1088821

Evanno, G., Regnaut, S., & Goudet, J. (2005). Detecting the number of clusters of individuals using the software STRUCTURE: A simulation study. *Molecular Ecology*, 14, 2611–2620. https://doi.org/10.1111/j.1365-294X.2005.02553.x

Excoffier, L., & Lischer, H. E. L. (2010). Arlequin suite ver 3.5: A new series of programs to perform population genetics analyses under Linux and Windows. *Molecular Ecology Resources*, 10, 564–567. https://doi.org/10.1111/j.1755-0998.2010.02847.x

Figueiredo, J. L., & Menezes, N. A. (1980). *Manual de peixes marinhos do sudeste do Brasil. III. Teleostei (2)*. Museu de Zoologia da USP. 90pp. Knapp 1951

Frankham, R., Bradshaw, C. J. A., & Brook, B. W. (2014). Genetics in conservation management: Revised recommendations for the 50/500 rules, red list criteria and population viability analyses. *Biological Conservation*, 170, 56–63. https://doi.org/10.1016/j.biocon.2013.12.036

Franks, J. S., Warren, J. R., & Buchanan, M. V. (1999). Age and growth of cobia, *Rachycentron canadum*, from the northeastern Gulf of Mexico. *Fishery Bulletin*, 97, 459–471. Available at: https://aquila.usm.edu/fac_pubs/4667/

Fratantoni, D. M., & Richardson, P. L. (2006). The evolution and demise of North Brazil Current rings. *Journal of Physical Oceanography*, 36(7), 1241–1264. https://doi.org/10.1175/JPO2907.1

Gary, S. F., Fox, A. D., Biastoch, A., Roberts, J. M., & Cunningham, S. A. (2020). Larval behaviour, dispersal and population connectivity in the deep sea. *Scientific Reports*, 10(1), 1–12. https://doi.org/10.1038/s41598-020-67503-7

Gold, J. R., Giresi, M. M., Renshaw, M. A., & Gwo, J. C. (2013). Population genetic comparisons among cobia from the northern Gulf of Mexico, U.S. Western Atlantic, and Southeast Asia. *North American Journal of Aquaculture*, 75(1), 57–63. https://doi.org/10.1080/15222055.2012.713899

Gopalakrishnan, G., Cornuelle, B. D., Hoteit, I., Rudnick, D. L., & Owens, W. B. (2013). State estimates and forecasts of the loop current in the Gulf of Mexico using the MITgcm and its adjoint. *Journal of Geophysical Research, Oceans*, 118(7), 3292–3314. https://doi.org/10.1002/jgrc.20239

Gordon, A. L. (1967). Circulation of the Caribbean Sea. *Journal of Geophysical Research*, 72(24), 6207–6223. https://doi.org/10.1029/JZ072i024p06207

Goudet, J. (2003). Fstat (ver. 2.9. 4), a program to estimate and test population genetics parameters. Updated from Goudet [1995]. Available at: http://www.unil.ch/izea/softwares/fstat.html

Gray, K. N., McDowell, J. R., Collette, B. B., & Graves, J. E. (2009). A molecular phylogeny of the remoras and their relatives. *Bulletin of Marine Science*, 84(2), 183–197.

Hamilton, S., Domingues, E. C., Júnior, R. B. P., Hazin, F. H. V., & Severi, W. (2021). Reproduction aspects of cobia caught in Pernambuco coast, northeastern Brazil. *Boletim Do Instituto de Pesca*, 47. https://doi.org/10.20950/1678-2305/bip.2021.47.e636

Huhn, F., Kameke, A. V., Allen-Perkins, S., Montero, P., Venâncio, A., & Pérez-Muñuzuri, V. (2012). Horizontal Lagrangian transport in a tidal-driven estuary - transport barriers attached to prominent coastal boundaries. *Continental Shelf Research*, 39, 1–13. https://doi.org/10.1016/j.csr.2012.03.005

Huhn, F., von Kameke, A., Pérez-Muñuzuri, V., Olascoaga, M. J., & Beron-Vera, F. J. (2012). The impact of advective transport by the South Indian Ocean countercurrent on the Madagascar plankton bloom. *Geophysical Research Letters*, 39, L06602. https://doi.org/10.1029/2012GL051246

Jombart, T. (2008). Adegenet: An R package for the multivariate analysis of genetic markers. *Bioinformatics*, 24(11), 1403–1405. https://doi.org/10.1093/bioinformatics/btn129

Jombart, T., Devillard, S., & Balloux, F. (2010). Discriminant analysis of principal components: A new method for the analysis of genetically

structured populations. *BMC Genetics*, 11(1), 94. https://doi.org/10.1186/1471-2156-11-94

Khoirunnisa, H., Wibowo, M., & Hendriyono, W. (2020). Determination of construction design to reduce the amount of marine litter at seawater intake using particle tracking module of numerical method by Mike 21 (case study: Tanjung Awar – Awar, Tuban, East Java). *Journal of Physics: Conference Series*, 1625, 012045. https://doi.org/10.1088/1742-6596/1625/1/012045

Knapp, F. T. (1951). Food habits of the sergeantfish, *Rachycentron canadus*. *Copeia*, 1, 101–102. https://doi.org/10.2307/1438092

Leis, J. M., van Herwerden, L., & Patterson, H. M. (2011). Estimating connectivity in marine fish populations: What works best? *Oceanography and Marine Biology*, 49, 193–234. https://doi.org/10.1201/b11009-6

Librado, P., & Rozas, J. (2009). DnaSP v5: A software for comprehensive analysis of DNA polymorphic data. *Bioinformatics*, 25, 1451–1452. https://doi.org/10.1093/bioinformatics/btp187

Lumpkin, R., Treguier, A., & Speer, K. (2002). Lagrangian eddy scales in the northern Atlantic Ocean. *Journal of Physical Oceanography*, 32(9), 2425–2440. https://doi.org/10.1175/1520-0485(2002)032%3C2425:LESITN%3E2.0.CO;2

Marcello, F., Wainer, I., & Rodrigues, R. R. (2018). South Atlantic subtropical gyre late twentieth century changes. *Journal of Geophysical Research*, *Oceans*, 123(8), 5194–5209. https://doi.org/10.1029/2018JC013815

Martins, N., Macagnan, L., Cassano, V., & Gurgel, C. (2021). Barriers to gene flow along the Brazilian coast: A synthesis and data analysis. *Authorea Preprints*. https://doi.org/10.22541/au.161358135.51187023/v1

Meyer, G. H., & Franks, J. S. (1996). Food of cobia *Rachycentron canadum* from the northcentral Gulf of Mexico. *Gulf Research Report*, 9, 161–167. https://doi.org/10.18785/grr.0903.02

Muller-Karger, F. E., McClain, C. R., & Richardson, P. L. (1988). The dispersal of the Amazon's water. *Nature*, 333, 56–59. https://doi.org/10.1038/333056a0

Napolitano, D. C., da Silveira, I. C. A., Tandon, A., & Calil, P. H. R. (2021). Submesoscale phenomena due to the Brazil current crossing of the Vitória-Trindade ridge. *Journal of Geophysical Research, Oceans*, 126(1), e2020JC016731. https://doi.org/10.1029/2020JC016731

Oosterhout, C. V., Weetman, D., & Hutchinson, W. F. (2006). Estimation and adjustment of microsatellite null alleles in nonequilibrium populations. *Molecular Ecology Resources*, 6(1), 255–256. https://doi.org/10.1111/j.1471-8286.2005.01082.x

Palumbi, S. R. (1994). Genetic divergence, reproductive isolation and marine speciation. *Annual Review of Ecology and Systematics*, 25, 547–572. https://doi.org/10.1146/annurev.es.25.110194.002555

Paquette, S. R. (2012). PopGenKit: Useful functions for (batch) file conversion and data resampling in microsatellite databases. R Package Version 1.0.

Peakall, R., & Smouse, P. E. (2006). GenAlEx 6: Genetic analysis in excel population genetics software for teaching and research. *Molecular Ecology Notes*, 6, 288–295. https://doi.org/10.1111/j.1471-8286.2005.01155.x

Pérez-Muñuzuri, V., & Huhn, F. (2010). The role of mesoscale eddies time and length scales on phytoplankton production. *Nonlinear Processes in Geophysics*, 17(2), 177–186. https://doi.org/10.5194/npg-17-177-2010

Perkinson, M., Darden, T., Jamison, M., Walker, M. J., Denson, M. R., Franks, J., Hendon, R., Musick, S., & Orbesen, E. S. (2019). Evaluation of the stock structure of cobia (*Rachycentron canadum*) in the southeastern United States by using dart-tag and genetics data. *Fishery Bulletin*, 117(3), 220–233. https://doi.org/10.7755/FB.117.3.9

Phinchongsakuldit, J., Chaipakdee, P., Collins, J. F., Jaroensutasinee, M., & Brookfield, J. F. Y. (2013). Population genetics of cobia (*Rachycentron canadum*) in the Gulf of Thailand and Andaman Sea: Fisheries

management implications. *Aquaculture International*, 21, 197–217. https://doi.org/10.1007/s10499-012-9545-1

Pineda, J., Hare, J. A., & Sponaugle, S. U. (2007). Larval transport and dispersal in the coastal ocean and consequences for population connectivity. *Oceanography*, 20(3), 22–39. Available at: https://www.jstor.org/stable/24860094. https://doi.org/10.5670/oceanog.2007.27

Pritchard, J. K., Stephens, M., & Donnelly, P. (2000). Inference of population structure using multilocus genotype data. *Genetics*, 155, 945–959. https://doi.org/10.1093/genetics/155.2.945

Pruett, C. L., Saillant, E., Renshaw, M. A., Patton, J. C., Rexroad, C. E., & Gold, J. R. (2005). Microsatellite DNA markers for population genetic studies and parentage assignment in cobia, *Rachycentron canadum*. *Molecular Ecology Notes*, 5, 84–86. https://doi.org/10.1111/j.1471-8286.2004.00840.x

R Core Team. (2020). R: a language and environment for statistical computing. R Foundation for Statistical Computing, Vienna, Austria. https://www.r-project.org/

Raymond, M., & Rousset, F. (1995). GENEPOP (version 1.2): Population genetics software for exact tests and ecumenicism. *Journal of Heredity*, 86, 248–249. https://doi.org/10.1093/oxfordjournals.jhered.a111573

Renshaw, M. A., Pruett, C. L., Saillant, E., Patton, J. C., Rexroad, C. E. III, & Gold, J. R. (2005). Microsatellite markers for cobia, *Rachycentron canadum*. *Gulf of Mexico Science*, 23, 248–251. https://doi.org/10.18785/goms.2302.11

Rice, W. R. (1989). Analyzing tables of statistical tests. *Evolution*, 43, 223–225. https://doi.org/10.2307/2409177

Rodrigues, R. R., Rothstein, L. M., & Wimbush, M. (2007). Seasonal variability of the south equatorial current bifurcation in the Atlantic Ocean: A numerical study. *Journal of Physical Oceanography*, 37, 16–30. https://doi.org/10.1175/JPO2983.1

Salze, G., Craig, S. R., Smith, B. H., Smith, E. P., & McLean, E. (2011). Morphological development of larval cobia *Rachycentron canadum* and the influence of dietary taurine supplementation. *Journal of Fish Biology*, 78(5), 1470–1491. https://doi.org/10.1111/j.1095-8649.2011.02954.x

Santos, S., Schneider, H., & Sampaio, I. (2003). Genetic differentiation of *Macrodon ancylodon* (Sciaenidae, Perciformes) populations in Atlantic coastal waters of South America as revealed by mtDNA analysis. *Genetics and Molecular Biology*, 26(2), 151–161. https://doi.org/10.1590/S1415-47572003000200008

Sá-Pinto, A., Branco, M. S., Alexandrino, P. B., Fontaine, M. C., & Baird, S. J. E. (2012). Barriers to gene flow in the marine environment: Insights from two common intertidal limpet species of the Atlantic and Mediterranean. *PLoS ONE*, 7(12), e50330. https://doi.org/10.1371/journal.pone.0050330

Sebille, E., Griffies, S., Abernathey, R., Adams, T., Berloff, P., Biastoch, A., Blanke, B., Chassignet, E., Cheng, Y., Cotter, C., Deleersnijder, E., Döös, K., Drake, H., Drijfhout, S., Gary, S., Heemink, A., Kjellsson, J., Koszalka, I., Lange, M., & Zika, J. (2018). Lagrangian ocean analysis: Fundamentals and practices. *Ocean Modelling*, 121, 49–75. https://doi.org/10.1016/j.ocemod.2017.11.008

Shaffer, R. V., Nakamura, E. L. (1989). Synopsis of biological data on the cobia *Rachycentron canadum* (Pisces: Rachycentridae). *NOAA Technical Reports*, National Marine Fisheries Service, 82, *FAO Fisheries Synopsis*, 153. Available at: https://aquadocs.org/handle/1834/20527

Smith, M. F., & Patton, J. L. (1993). The diversification of South American murid rodents: Evidence from mitochondrial DNA sequence data for the akodontine tribe. *Biological Journal of the Linnean Society*, 50, 149–177. https://doi.org/10.1111/j.1095-8312.1993.tb00924.x

Sousa, M., Decastro, M., Gago, J., Ribeiro, A., Des, M., Gómez-Gesteira, J., Dias, J., & Gomez-Gesteira, M. (2021). Modelling the distribution of microplastics released by wastewater treatment plants in Ria de Vigo (NW Iberian Peninsula). *Marine Pollution Bulletin*, 166, 112227. https://doi.org/10.1016/j.marpolbul.2021.112227

Tamura, K., Peterson, D., Peterson, N., Stecher, G., Nei, M., & Kumar, S. (2011). MEGA5: Molecular evolutionary genetics analysis using maximum likelihood, evolutionary distance, and maximum parsimony methods. *Molecular Biology and Evolution, 28*, 2731–2739. https://doi.org/10.1093/molbev/msr121

Thompson, J. D., Higgins, D. G., & Gibson, T. J. (1994). CLUSTAL W: Improving the sensitivity of progressive multiple sequence alignment through sequence weighting, position specific gap penalties and weight matrix choice. *Computer Applications in Biological Sciences, 10*, 19–29. https://doi.org/10.1093/nar/22.22.4673

Truelove, N. K., Kough, A. S., Behringer, D. C., Paris, C. B., Box, S. J., Preziosi, R. F., & Butler, M. J. (2017). Biophysical connectivity explains population genetic structure in a highly dispersive marine species. *Coral Reefs, 36*(1), 233–244. https://doi.org/10.1007/s00338-016-1516-y

Waples, R. S., & Do, C. (2010). Linkage disequilibrium estimates of contemporaryNeusing highly variable genetic markers: A largely untapped resource for applied conservation and evolution. *Evolutionary Applications, 3*(3), 244–262. Portico. https://doi.org/10.1111/j.1752-4571.2009.00104.x

Welsh, S. E., & Masamichi, I. (2000). Loop current rings and the deep circulation in the Gulf of Mexico. *Journal of Geophysical Research, Oceans, 105*(C7), 16951–16959. https://doi.org/10.1029/2000JC900054

SUPPORTING INFORMATION

Additional supporting information can be found online in the Supporting Information section at the end of this article.